Electronic Supplementary Information

Facile Fabrication in Coordination Networks: An *in Situ* Sequential Replacement of Linkers by Successive SC-SC Transformations *via* Core@Shell Crystals

Bahare Ebrahimi and Behrouz Notash*

Department of Inorganic Chemistry, Shahid Beheshti University, 1983969411, Tehran, Iran.

E-mail: b_notash@sbu.ac.ir; Fax: +98 2122431663; Tel: +98 2129904363

Content

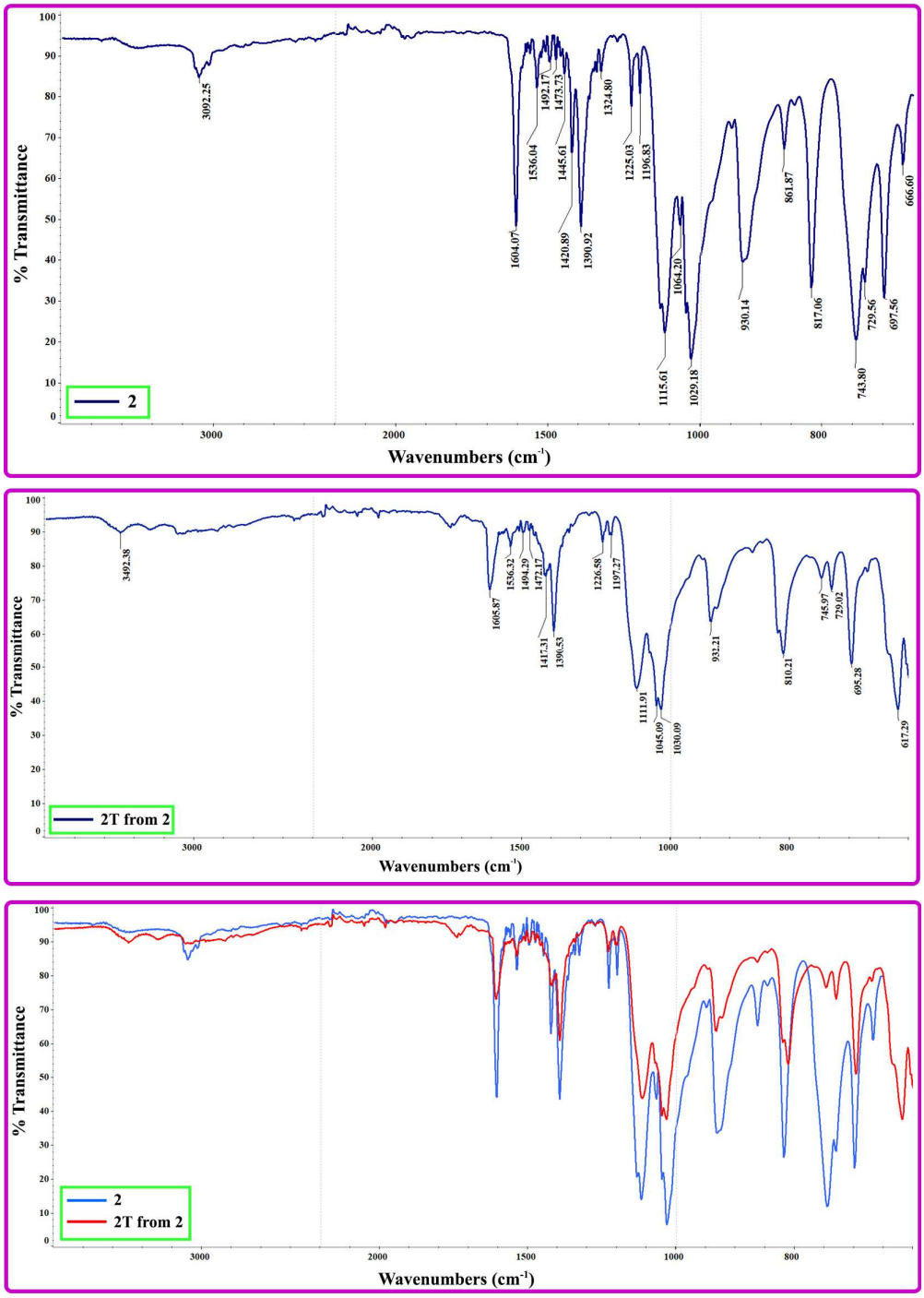

Fig. S1 ATR spectrum of compound **2** and **2T** recorded after transformation from **2** to **2T**.

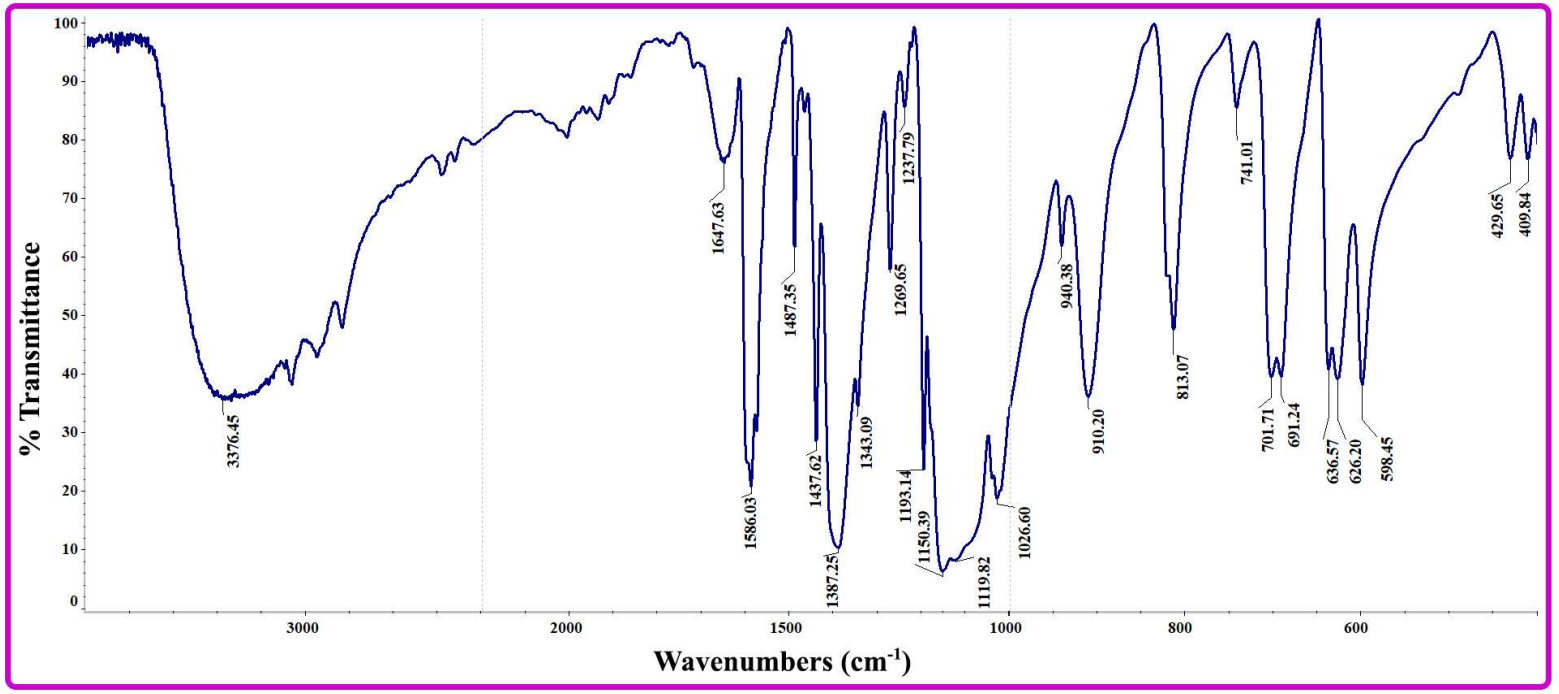

Fig. S2 FT-IR spectrum of compound **3** in KBr recorded after structural transformation from **2** to **3**.

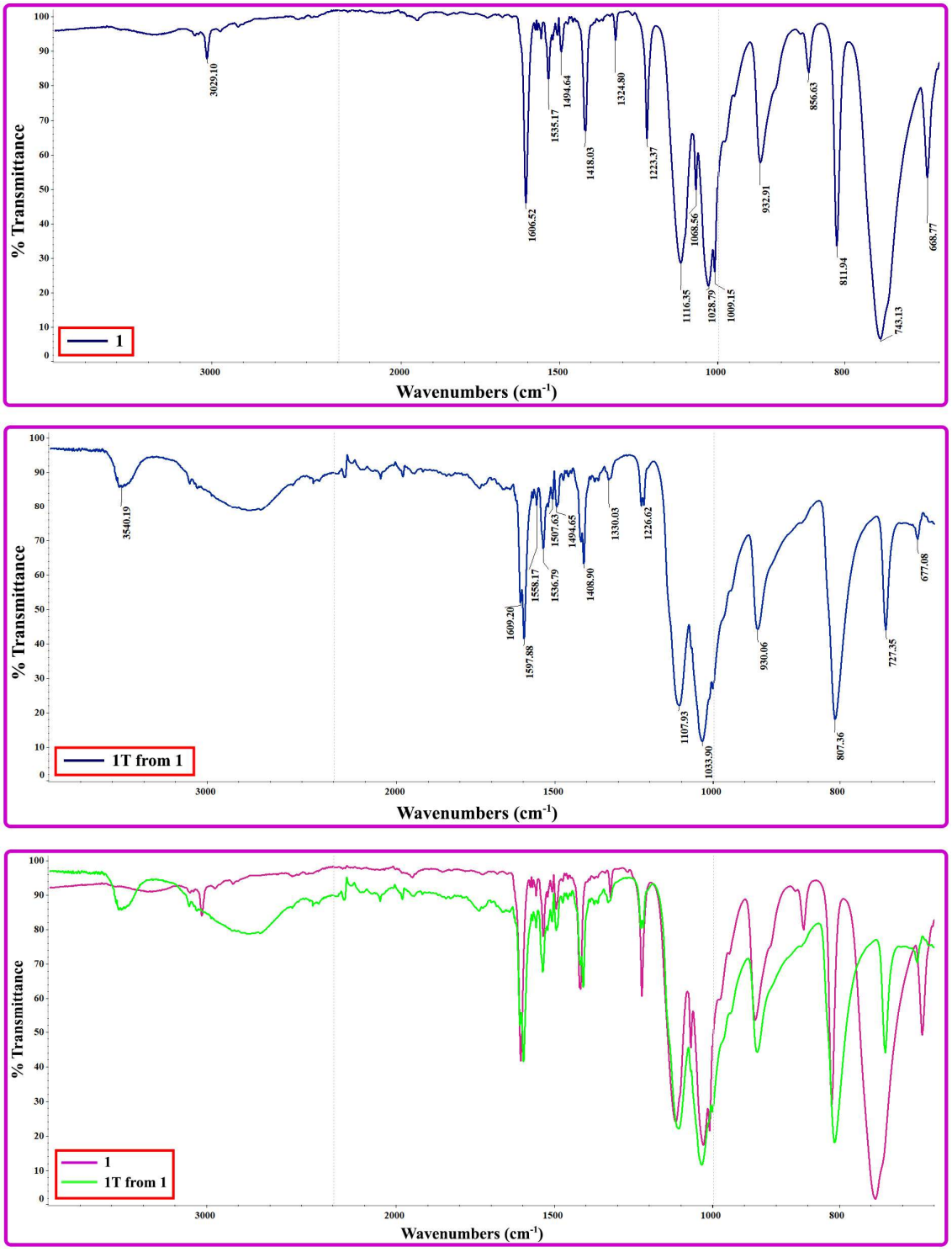

Fig. S3 ATR spectrum of compound **1** and **1T** recorded after transformation from **1** to **1T**.

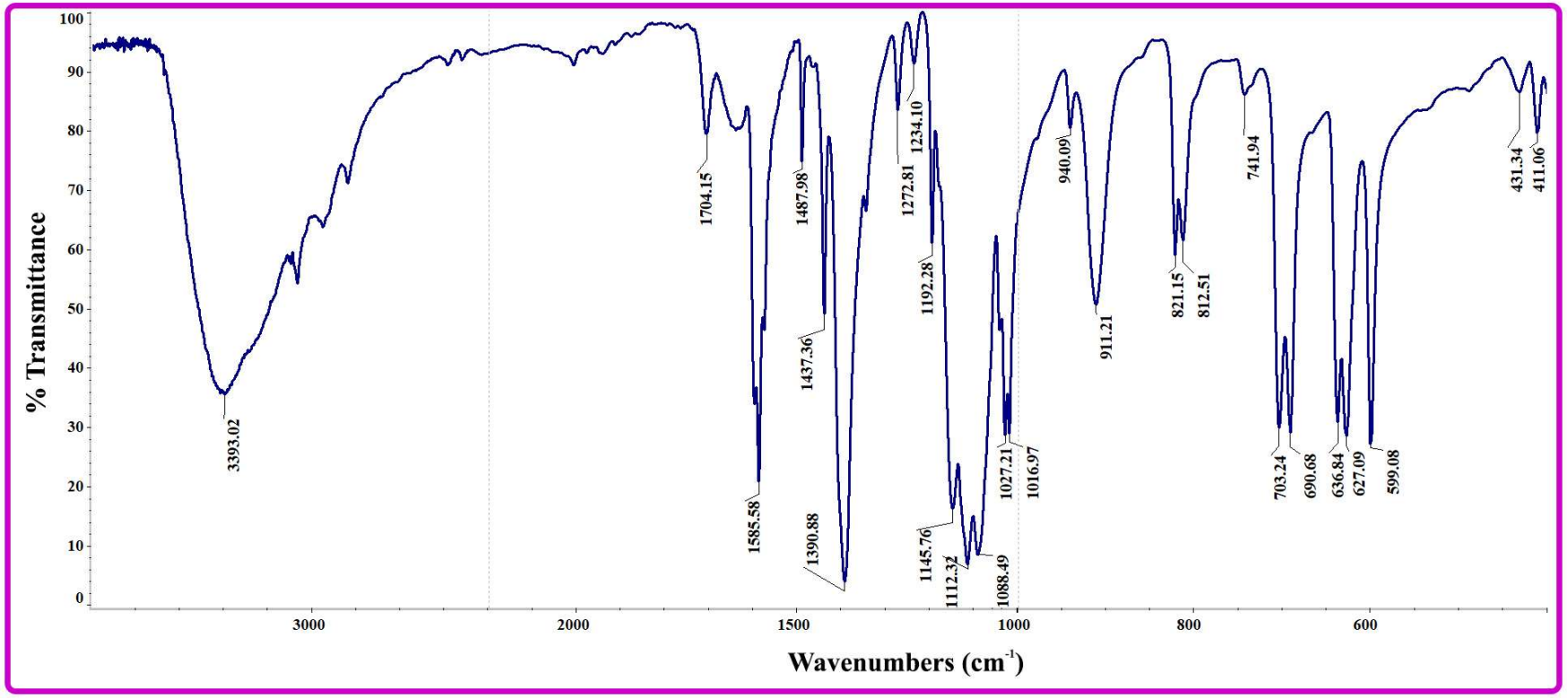

Fig. S4 FT-IR spectrum of compound **3** in KBr.

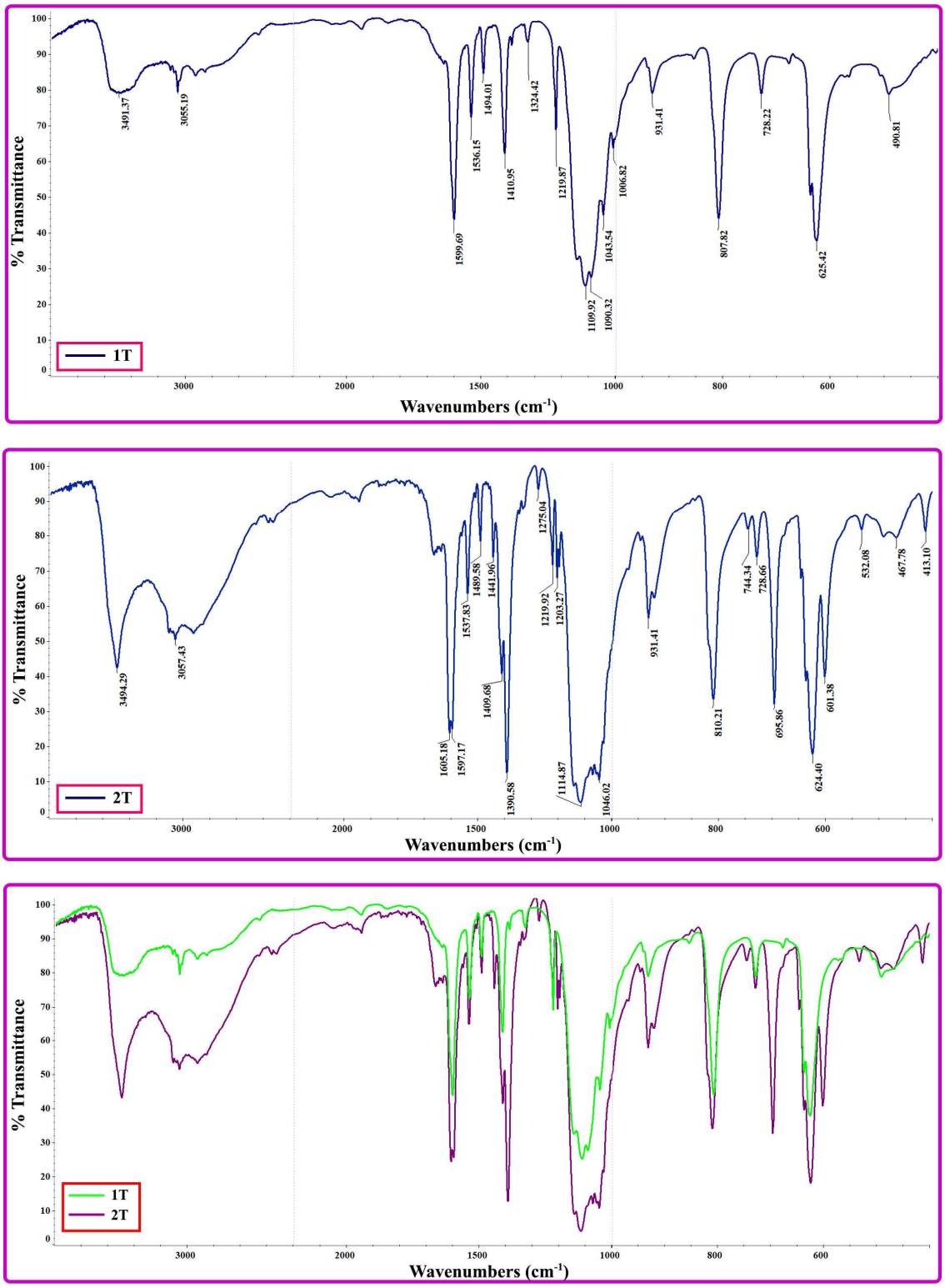

Fig. S5 FT-IR spectrum for compounds **1T** and **2T** in KBr recorded after transformation from **1** and **2** to **1T** and **2T**.

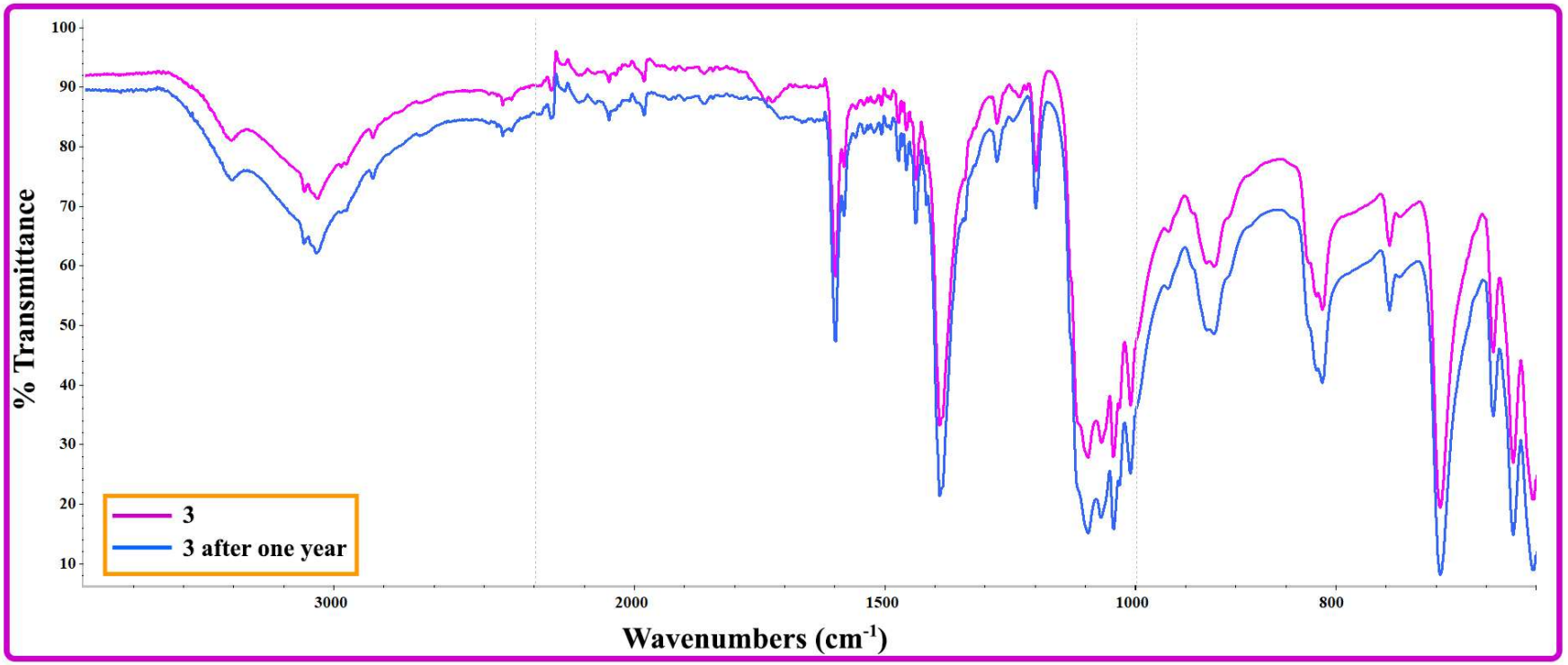

Fig. S6 ATR spectrum for crystal of **3** and powder of **3** after one year.

Scheme S1. Two Possible Proposed Structures for Polymeric Structures of Compound {[Cd(3,3′-pytz)(H_2O)$_2$(ClO_4)$_2$](4,4′-bipy)}n= ∞ (2T) Generated by the Structure of Compound 2 in Mercury Software. a) Free 4,4′-bipy Ligands. b) Free 3,3′-pytz Ligands

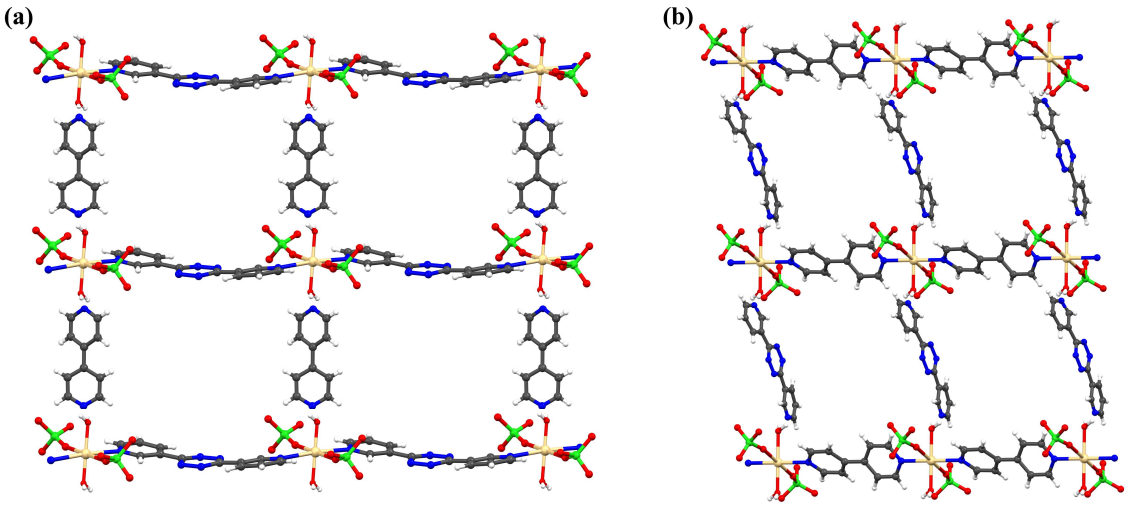

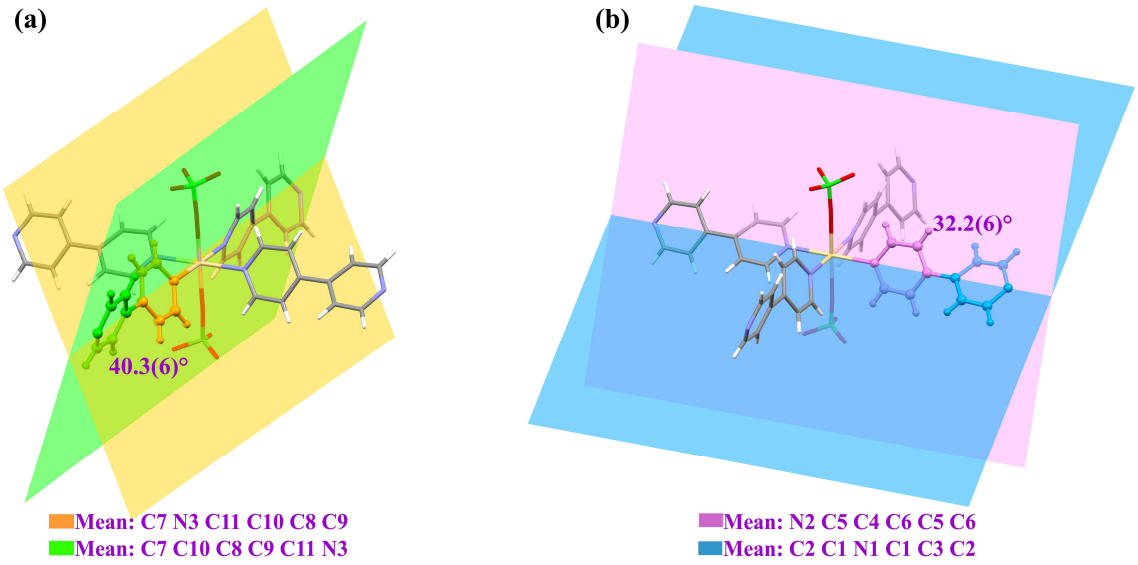

Fig. S7 (a, b) Angle between mean planes of two pyridine rings of 4,4′-bipy ligands in **1**.

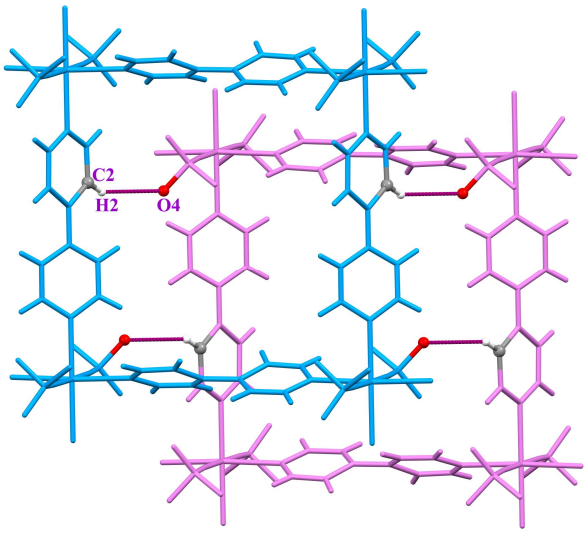

Fig. S8 View of the hydrogen-bonding interactions between adjacent 2D square-grid layers in **1**.

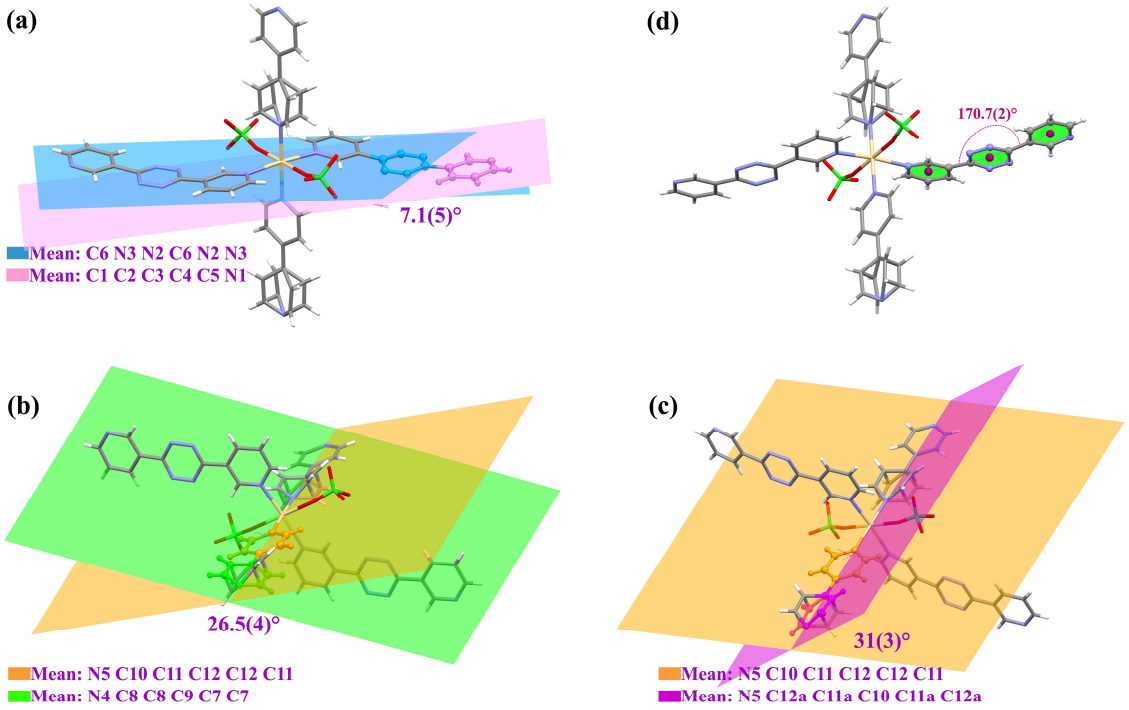

Fig. S9 (a) Angle between mean planes of the side pyridine rings and the central tetrazine ring of the 3,3′-pytz linker and (b, c) angle between mean planes of the pyridine rings of 4,4′-bipy linker and (d) Cg $_{pyridine}$-Cg $_{tetrazine}$-Cg $_{pyridine}$ angle of the 3,3′-pytz linker in **2**.

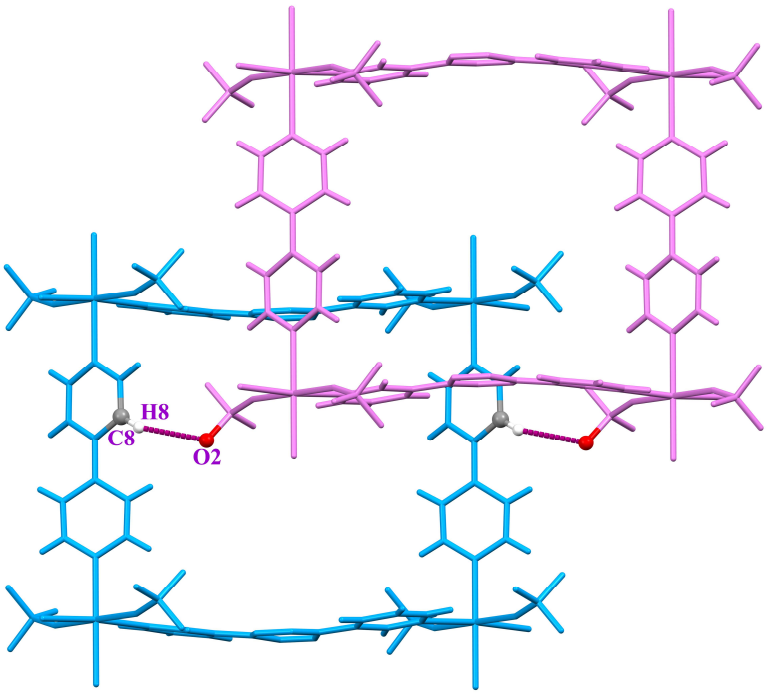

Fig. S10 View of the hydrogen-bonding interactions between adjacent 2D rectangular-grid layers in **2**. For more clarity, disorder of pyridine ring of 4,4′-bipy linker is omitted.

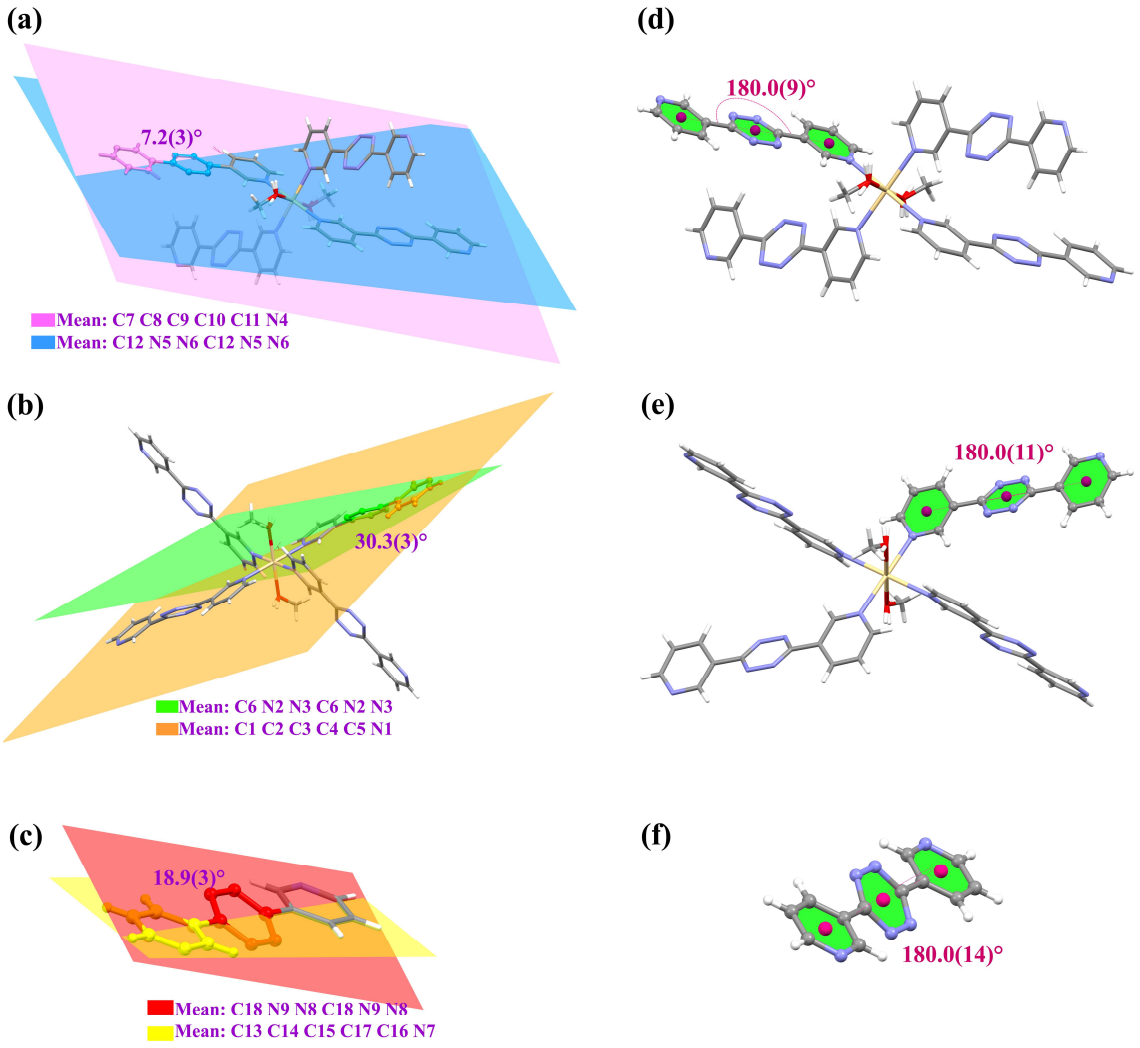

Fig. S11 (a, b) Angle between mean planes of the side pyridine rings and the central tetrazine ring of the coordinated ligand. (c) Angles between mean planes of the side pyridine ring and the central tetrazine ring of the co-crystalized ligand. (d, e, f) Angle of Cg···Cg···Cg of the pyridine and tetrazine rings of coordinated and co-crystalized 3,3′-pytz ligands in **3**.

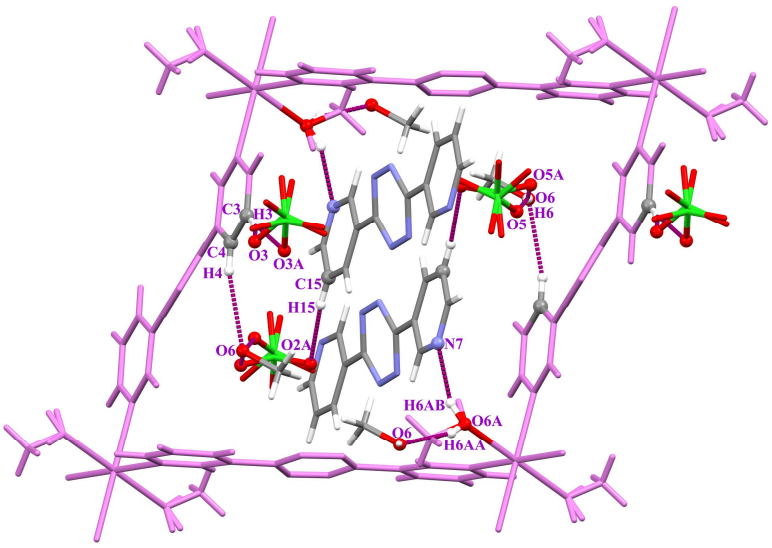

Fig. S12 View of the hydrogen-bonding interactions in **3**.

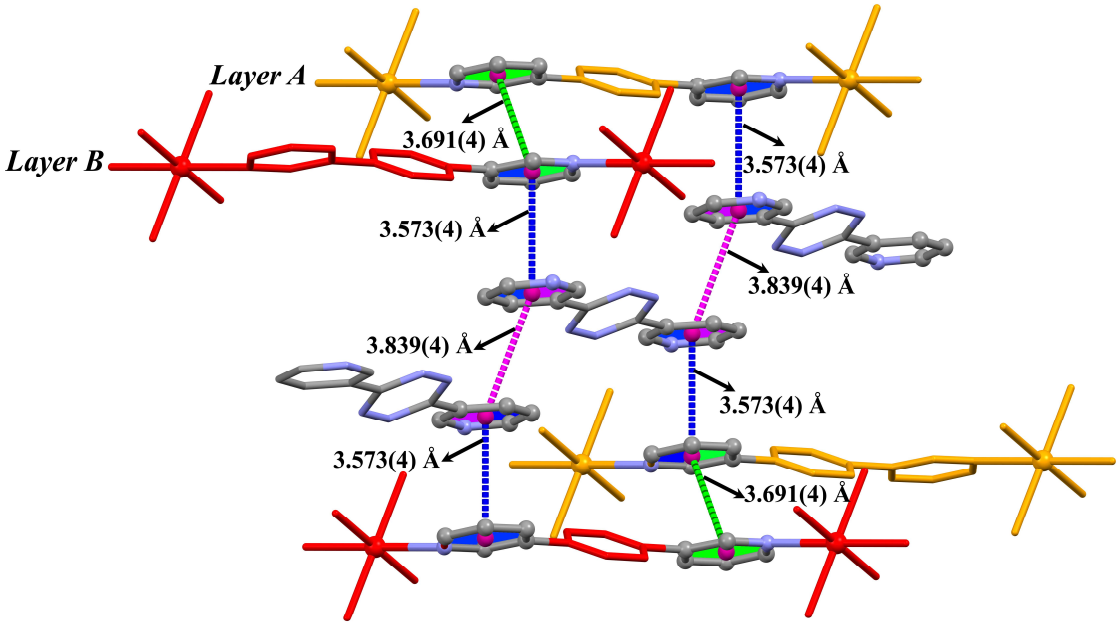

Fig. S13 View of the π-π interactions between pyridine rings of coordinated and co-crystalized 3,3′-pytz ligands in **3**.

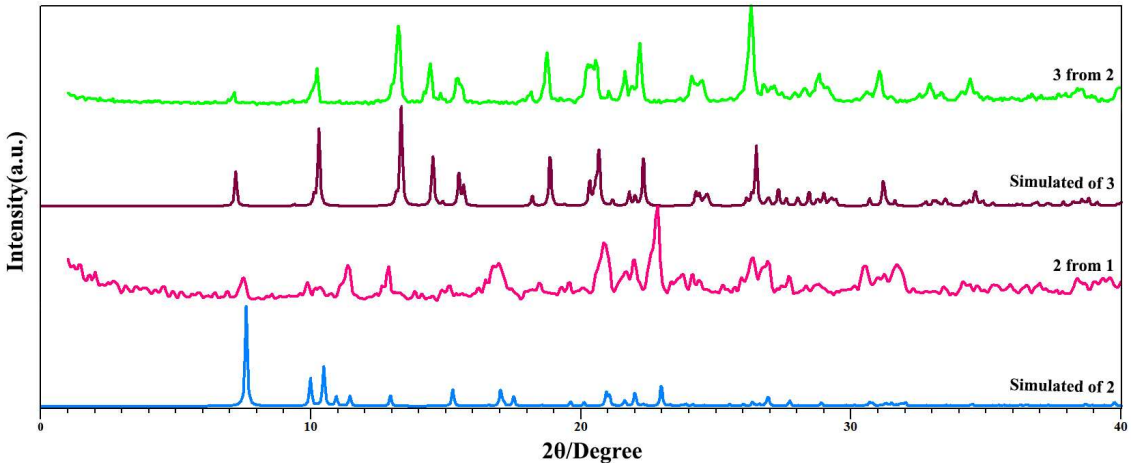

Fig. S14 PXRD pattern of structural transformation of compounds **1** to **2** and **2** to **3**.

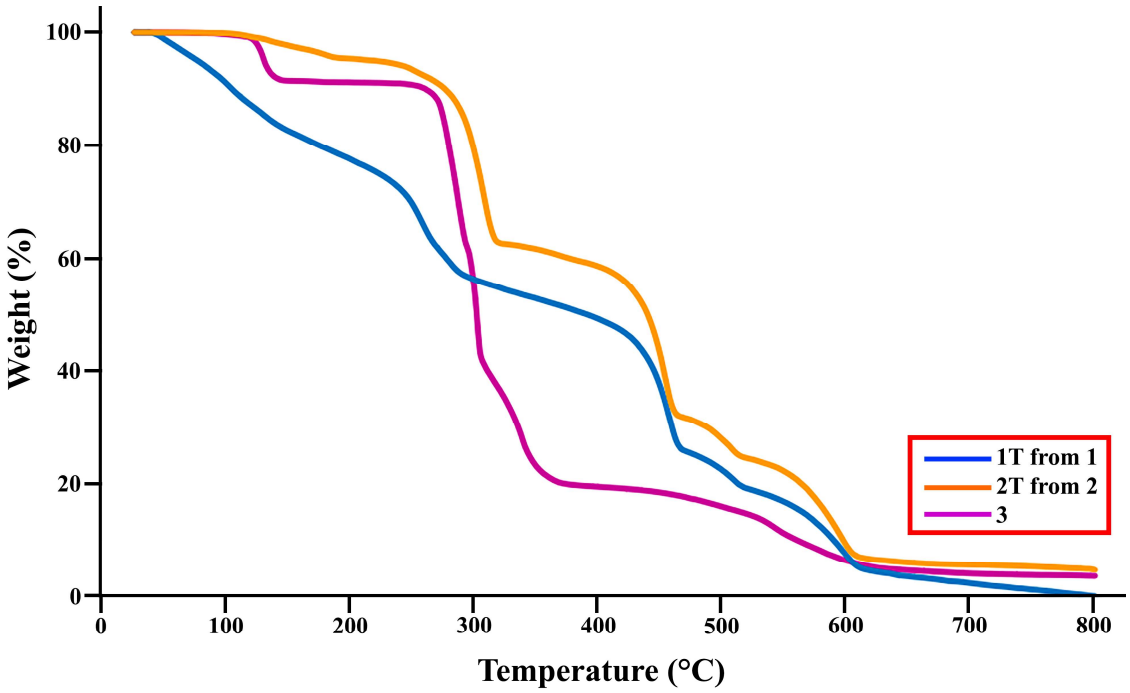

Fig. S15 TGA curves for compounds **1T**, **2T** and **3**.

Table S1. Selected bond lengths (Å) and angles (deg) for **1**.

Cd(1)-O(1)	2.339(9)	N(1)-Cd(1)-N(3)	91.50(17)
Cd(1)-N(1)	2.307(11)	N(1)-Cd(1)-N(2)$^{\#1}$	180.0
Cd(1)-N(3)	2.329(10)	O(1)$^{\#2}$-Cd(1)-N(1)	90.3(2)
Cd(1)-N(2)$^{\#1}$	2.333(9)	N(1)-Cd(1)-N(3)$^{\#2}$	91.50(17)
Cd(1)-O(1)$^{\#2}$	2.339(9)	N(2)$^{\#1}$-Cd(1)-N(3)	88.50(17)
Cd(1)-N(3)$^{\#2}$	2.329(10)	O(1)$^{\#2}$-Cd(1)-N(3)	88.3(4)
O(1)-Cd(1)-N(1)	90.3(2)	N(3)-Cd(1)-N(3)$^{\#2}$	177.0(2)
O(1)-Cd(1)-N(3)	91.7(4)	O(1)$^{\#2}$-Cd(1)-N(2)$^{\#1}$	89.7(2)
O(1)-Cd(1)-N2$^{\#1}$	89.7(2)	N(2)$^{\#1}$-Cd(1)-N(3)$^{\#2}$	88.50(17)
O(1)-Cd(1)-O(1)$^{\#2}$	179.3(3)	O(1)$^{\#2}$-Cd(1)-N(3)$^{\#2}$	91.7(4)
O(1)-Cd(1)-N(3)$^{\#2}$	88.3(4)		

Symmetry codes: #1: x, y-1, z; #2: 1-x, y, 1/2-z.

Table S2. Selected bond lengths (Å) and angles (deg) for **2**.

Cd(1)-O(1)	2.351(6)	N(1)-Cd(1)-N(4)	87.46(17)
Cd(1)-N(1)	2.362(6)	N(1)-Cd(1)-N(5)$^{\#1}$	92.54(17)
Cd(1)-N(4)	2.298(9)	O(1)$^{\#2}$-Cd(1)-N(1)	92.1(2)
Cd(1)-N(5)$^{\#1}$	2.270(9)	N(1)-Cd(1)-N(1)$^{\#2}$	174.9(2)
Cd(1)-O(1)$^{\#2}$	2.351(6)	N(4)-Cd(1)-N(5)$^{\#1}$	180.0
Cd(1)-N(1)$^{\#2}$	2.362(6)	O(1)$^{\#2}$-Cd(1)-N(4)	89.91(17)
O(1)-Cd(1)-N(1)	87.9(2)	N(1)$^{\#2}$-Cd(1)-N(4)	87.46(17)
O(1)-Cd(1)-N(4)	89.91(17)	O(1)$^{\#2}$-Cd(1)-N(5)$^{\#1}$	90.09(17)
O(1)-Cd(1)-N(5)$^{\#1}$	90.09(17)	N(1)$^{\#2}$-Cd(1)-N(5)$^{\#1}$	92.54(17)
O(1)-Cd(1)-O(1)$^{\#2}$	179.8(3)	O(1)$^{\#2}$-Cd(1)-N(1)$^{\#2}$	87.9(2)
O(1)-Cd(1)-N(1)$^{\#2}$	92.1(2)		

Symmetry codes: #1: x, -1+y, z; #2: **1/2-x, y, 1/2-z**.

Table S3. Selected bond lengths (Å) and angles (deg) for **3**.

Cd(1)-O(6A)	2.338(5)	N(1)-Cd(1)-N(4)	88.75(18)
Cd(1)-N(1)	2.366(5)	O(6A)$^{\#1}$-Cd(1)-N(1)	99.07(17)
Cd(1)-N(4)	2.364(5)	N(1)-Cd(1)-N(1)$^{\#1}$	180.0
Cd(1)-O(6A)$^{\#1}$	2.338(5)	N(1)-Cd(1)-N(4)$^{\#1}$	91.25(18)
Cd(1)-N(1)$^{\#1}$	2.366(5)	O(6A)$^{\#1}$-Cd(1)-N(4)	90.54(17)
Cd(1)-N(4)$^{\#1}$	2.364(5)	N(1)$^{\#1}$-Cd(1)-N(4)	91.25(18)
O(6A)-Cd(1)-N(1)	80.93(17)	N(4)-Cd(1)-N(4)$^{\#1}$	180.0
O(6A)-Cd(1)-N(4)	89.46(17)	O(6A)$^{\#1}$-Cd(1)-N(1)$^{\#1}$	80.93(17)
O(6A)-Cd(1)-O(6A)$^{\#1}$	180.0	O(6A)$^{\#1}$-Cd(1)-N(4)$^{\#1}$	89.46(17)
O(6A)-Cd(1)-N(1)$^{\#1}$	99.07(17)	N(1)$^{\#1}$-Cd(1)-N(4)$^{\#1}$	88.75(18)
O(6A)-Cd(1)-N(4)$^{\#1}$	90.54(17)		

Symmetry code: #1: 1-x+,1-y,1-z.

Table S4. Hydrogen-bonding parameters (D–H···A) for **1-3**.

Compound	D–H···A	D–H/Å	H···A/Å	D···A/Å	DHA/deg
1[a]	C(2)–H(2)···O(4)$^{\#1}$	0.929(16)	2.546(17)	3.337(16)	143.2(15)
2[b]	C(8)–H(8)···O(2)$^{\#1}$	0.930(10)	2.593(13)	3.455(13)	154.5(8)
3[c]	O(6A)–H(6AA)···O(6)	0.85(7)	1.86(7)	2.631(10)	150(7)
	O(6A)–H(6AB)···N(7)	0.85(5)	2.07(5)	2.873(8)	159(6)
	O(6)–H(6)···O(5)$^{\#1}$	0.82(8)	1.75(12)	2.55(3)	162(14)
	O(6)–H(6)···O(5A)$^{\#1}$	0.82(8)	2.01(8)	2.82(2)	168(15)
	C(3)–H(3)···O(3)$^{\#2}$	0.930(9)	2.419(15)	3.310(15)	160.2(8)
	C(3)–H(3)···O(3A)$^{\#2}$	0.930(9)	2.305(19)	3.231(18)	173.9(8)
	C(4)–H(4)···O(6)$^{\#3}$	0.930(9)	2.572(11)	3.475(11)	164.0(7)
	C(15)–H(15)···O(2A)$^{\#4}$	0.931(12)	2.46(2)	3.32(2)	153.8(10)

[a]Symmetry code: #1: 1-x, -y, -z. [b]Symmetry code: #1: -x, 1-y, -z. [c]Symmetry code: #1: -x, 1-y, 1-z; #2: 1-x, 2-y, 1-z; #3: x, 1+y, z; #4: -x, 2-y, 1-z.

Infrared spectroscopy studies. The ATR spectrum of freshly prepared single crystals of **1** indicated the stretching vibration of C=N of 4,4′-bipy at 1606 cm^{-1} and peak at 1116 cm^{-1} corresponded to Cl–O group of perchlorate anion (Fig. S3).[1] In addition, a band related to C–Cl group of chloroform molecule was observed at 743 cm^{-1} in compound **1**.[2] Also, the ATR spectrum of freshly synthesized single crystals of **2** is depicted in Fig. S1. The sharp peaks at 1390 cm^{-1} and 1604 cm^{-1} in compound **2** are assigned to the stretching vibration of N=N and C=N groups of 3,3′-pytz and 4,4′-bipy ligands and peak at 743 cm^{-1} related to absorption band of chloroform molecule.[1, 3] The absorption band of Cl–O group of perchlorate anion appeared at 1115 cm^{-1} for **2**.[1] The peak observed at 1060 cm^{-1} can be attributed to the stretching frequency of C–O of methanol molecule in **3**.[2] The sharp absorption band at 1387 cm^{-1} and 1586 cm^{-1} in FT-IR spectra of compound **3** related to N=N and C=N groups of 3,3′-pytz ligand (Fig. S2).[1, 3] The broad band of O–H group of a water molecule is at 3376 cm^{-1} in **3**. The peak at 1112 cm^{-1} can be identified as the stretching frequency of Cl–O groups of perchlorate anion in compound **3**.[1] As indicated in Fig. S6, compound **3** is completely stable in environment and the absorption band at 1068 cm^{-1} and 3068 cm^{-1} can be corresponded to the stretching frequency of C–O and O–H of methanol molecule, respectively. Therefore, the removal of methanol molecules does not happen in compound **3** and this compound has good stability in air.

In addition, after transformation from compounds **1** and **2** to **1T** and **2T**, the stretching vibration of O–H group of coordinated water molecules appeared at 3400 cm^{-1}, respectively (Fig. S5). As shown in Fig. S3, the stretching vibration of C=N of coordinated 4,4′-bipy linker in compound **1** appears at 1606 cm^{-1}, and the peaks at 1597 cm^{-1} and 1609 cm^{-1} related to stretching vibration of C=N of free and coordinated 4,4′-bipy in **1T**,

respectively. As depicted in Fig. S5, the appearance of the absorption band at 1597 cm^{-1} corresponded to stretching vibration of C=N of free 4,4′-bipy in **2T**. According to the comparison of IR, we suggest that structure of compound **2T** contains free 4,4′-bipy linkers and coordinated 3,3′-pytz linkers and this structural form is more probable. (Scheme S1a).

Crystallographic Structure Determination

Single crystals of compounds **1**-**3** were mounted with grease at the top of glass fiber for data collection. In the case of compounds **1** and **2**, single crystals were covered by glue to protect them from air. The X-ray diffraction data of suitable single crystals were carried out on a STOE IPDS-II diffractometer at 298(2) K, that was equipped with a graphite-monochromated Mo-Kα (λα = 0.71073 Å) radiation source. All data were collected to a maximum 2θ value of 24.999°, 24.996°, and 25.000° for single crystals of **1**-**3**, respectively. Diffraction data were collected in a series of ω scans in 1° oscillation and integrated using the Stoe X-AREA[4] software package. X-RED[5] and X-SHAPE[6] software was used for numerical absorption correction. The data were corrected for Lorentz and polarizing effects. Crystal structures were solved by direct methods[7] and analysis of subsequent difference Fourier maps and then refined on F^2 using a full-matrix least-squares procedure with anisotropic displacement parameters.[8] Atomic factors are taken from the International Tables for X-ray Crystallography.[9] All refinements were performed using the X-STEP32 crystallographic software package.[10] The SQUEEZE function was applied for compounds **1** and **2**, due to lattice solvent molecules were highly disordered in the framework. Further details for crystallographic data and structure refinement parameters for compounds **1**-**3** are listed in Table 1. Selected bond lengths and angles are collected in Tables S1-S3.

References:

1 K. Nakamoto, *Infrared and Raman Spectra of Inorganic and Coordination Compounds, Part B: Applications in Coordination, Organometallic, and Bioinorganic Chemistry*. Wiley: 2009.
2 D. L. Pavia, G. M. Lampman, G. S. Kriz and J. A. Vyvyan, *Introduction to Spectroscopy*. Cengage Learning: 2014.
3 P. Patnaik, *Dean's Analytical Chemistry Handbook*. 2nd ed. ed.; McGraw-Hill Education: New York, 2004.
4 X–AREA: program for the acquisition and analysis of data, Version 1.30, Darmatadt, Germany. 2005.
5 X-RED: Program for data reduction and absorption correction, Version 1.28 b, Darmstadt, Germany. 2005.
6 X-SHAPE:, Program for Crystal Optimization for Numerical Absorption Correction, version 2.05 Darmstadt, Germany (Stoe & Cie GmbH:), 2004.
7 Sheldrick, G. M., SHELXS-97; Program for Crystal Structure Solution. University of Göttingen: Göttingen, Germany: 1997.

8 L. J. Bourhis, O. V. Dolomanov, R. J. Gildea, J. A. K. Howard and H. Puschmann, *Refinement engine olex2.refine: The anatomy of a comprehensive constrained, restrained refinement program for the modern computing environment – Olex2 dissected.* Acta Crystallogr. Sect. A, 2015, **71**, 59-75.
9 International Tables for X-ray Crystallography, V. C., Dordrecht, The Netherlands, Kluwer Academic Publisher: , 1995.
10 X-STEP32, Crystallographic Package, version 1.07 b, Darmstadt, Germany. 2000.